

Dalton Transactions

Accepted Manuscript



This is an *Accepted Manuscript*, which has been through the Royal Society of Chemistry peer review process and has been accepted for publication.

Accepted Manuscripts are published online shortly after acceptance, before technical editing, formatting and proof reading. Using this free service, authors can make their results available to the community, in citable form, before we publish the edited article. We will replace this *Accepted Manuscript* with the edited and formatted *Advance Article* as soon as it is available.

You can find more information about *Accepted Manuscripts* in the [Information for Authors](#).

Please note that technical editing may introduce minor changes to the text and/or graphics, which may alter content. The journal's standard [Terms & Conditions](#) and the [Ethical guidelines](#) still apply. In no event shall the Royal Society of Chemistry be held responsible for any errors or omissions in this *Accepted Manuscript* or any consequences arising from the use of any information it contains.

***S*-Shaped Decanuclear Heterometallic [Ni₈Ln₂] Complexes [Ln(III)
= Gd, Tb, Dy and Ho]: Theoretical Modeling of the Magnetic
Properties of the Gadolinium Analogue**

*Sakiat Hossain,^a Sourav Das,^a Amit Chakraborty,^a Francesc Lloret,^{*b} Joan Cano,^b Emilio Pardo^b
and Vadapalli Chandrasekhar^{*a,c}*

^aDepartment of Chemistry, Indian Institute of Technology Kanpur, Kanpur-208016, India

^bDepartament de Química Inorgànica, Instituto de Ciencia Molecular (ICMOL), Universitat de
València, 46980 Paterna, València, Spain

^cNational Institute of Science Education and Research, Institute of Physics Campus, Sachivalaya
Marg, Sainik School Road, Bhubaneswar-751 005, Odisha, India

AUTHOR EMAIL ADDRESS: vc@iitk.ac.in (VC), francisco.lloret@uv.es (F.L)

Abstract

The reaction of 8-quinolinol-2-carboaldoxime (LH_2) with Ni^{II} and Ln^{III} salts afforded the heterometallic decanuclear compounds $[\text{Ni}_8\text{Dy}_2(\mu_3\text{-OH})_2(\text{L})_8(\text{LH})_2(\text{H}_2\text{O})_6](\text{ClO}_4)_2 \cdot 16\text{H}_2\text{O}$ (**1**), $[\text{Ni}_8\text{Gd}_2(\mu_3\text{-OH})_2(\text{L})_8(\text{LH})_2(\text{H}_2\text{O})_4(\text{MeOH})_2](\text{NO}_3)_2 \cdot 12\text{H}_2\text{O}$ (**2**), $[\text{Ni}_8\text{Ho}_2(\mu_3\text{-OH})_2(\text{L})_8(\text{LH})_2(\text{H}_2\text{O})_4(\text{MeOH})_2](\text{ClO}_4)_2 \cdot 2\text{MeOH} \cdot 12\text{H}_2\text{O}$ (**3**) and $[\text{Ni}_8\text{Tb}_2(\mu_3\text{-OH})_2(\text{L})_8(\text{LH})_2(\text{MeOH})_4(\text{OMe})_2] \cdot 2\text{CH}_2\text{Cl}_2 \cdot 8\text{H}_2\text{O}$ (**4**). While compounds **1-3** are dicationic, compound **4** is neutral. These compounds possess an *S-shaped* architecture and comprise a long chain of metal ions bound to each other. In all the complexes, the eight Ni^{II} and two Ln^{III} ions of the multimetallic ensemble are held together by two $\mu_3\text{-OH}$, eight dianionic (L^{2-}) and two monoanionic oxime ligands (LH^-) whereas compound **4** has two $\mu_3\text{-OH}$, eight dianionic (L^{2-}), two monoanionic oxime ligands (LH^-) and two terminal methoxy (MeO^-) ligands. The central portion of the *S-shaped* molecular wire is made up of an octanuclear Ni^{II} ensemble which has at its two ends the Ln^{III} caps. Magnetic studies on **1-4** reveal that the magnetic interactions between neighboring metal ions are negligible at room temperature. On the other hand, at lower temperatures in all the compounds anti-ferromagnetic interactions seem to be dominated. Analysis of the magnetic data for the Gd^{III} derivative indicates $\text{Ni}^{\text{II}}\text{-Ni}^{\text{II}}$ anti-ferromagnetic interactions and $\text{Gd}^{\text{III}}\text{-Ni}^{\text{II}}$ ferromagnetic interactions at low temperatures. A theoretical density functional (*DF*) study on the magnetic behavior of the Gd^{III} derivative suggests that while the weak ferromagnetic interaction between Gd^{III} and Ni^{II} is in line with the expectation of the magnetic interactions between orthogonal d and f orbitals, antiferromagnetic $\text{Ni}^{\text{II}}\text{-Ni}^{\text{II}}$ interactions are related to the wide Ni-O-Ni angles ($\sim 102^\circ$) and quasi-planar conformation of the Ni_2O_2 core.

Keywords: Heterometallic complexes; 3d/4f complexes; Ni^{II}/Ln^{III} complexes; DFT studies; anti-ferromagnetic interactions; ferromagnetic interactions

INTRODUCTION

There is a great deal of contemporary interest in the synthesis, structure and property evaluation of molecular multimetallic ensembles.¹ This interest emanates from several points of view. From the point of view of chemical synthesis, such ensembles represent a challenge. Ligand design is of critical importance and can tip the balance between the formation of compounds that can possess extended structures or those that are molecular entities.² The process of such synthesis also leads, in some instances, to aesthetically pleasing molecular structures. Knowledge of assembling discrete multi-metal assemblies will prove crucial in several areas, for example, in the preparation of short molecular wires that can be used in nanodevices.³ Second, molecular multi-metal assemblies can be viewed as possible model compounds for heterogeneous metal-containing surfaces.⁴ Third, the close proximity of metal ions within molecular multi-metallic ensembles allows the phenomenon of molecular magnetism to be investigated.⁵ In this regard, apart from the nature of metal ions that are present in the compound, the type of linkage (single atom/multi atom; nature of the linking atom) that exist between such metal ions and consequently the inter-metal ion orientation, is crucial for determining the overall magnetic behavior of such architectures including the possibility of realizing molecular magnets.⁶

As mentioned above, one of the most important factors that can contribute to the successful realization of molecular multi-metallic assemblies is ligand design. While it is fairly straightforward to achieve the assembly of mono nuclear compounds or multi-nuclear compounds possessing extended structures, it is still quite challenging to isolate discrete molecular entities containing several metal ions; properly designed ligands have to be utilized for this purpose. From among the many families of multi-site coordination ligands that have been investigated thus far, oxime ligands seem to be quite appropriate for being used in poly nuclear

metal chemistry. 2-Pyridyl oxime⁷, 2-hydroxybenzaldehyde oxime⁸ and 2,6-diacetylpyridine-dioxime⁹ are among those ligands that have been widely used to afford structurally and magnetically interesting homo- and heterometallic 3d-4f complexes. These oximes possess multiple coordination sites: for example, 2-pyridyl oxime, functions as a bidentate ligand in its neutral form and as a tridentate ligand in its anionic form. On the other hand, 2,6-diacetylpyridine dioxime is a tridentate ligand in its neutral form and pentadentate in its anionic form. In view of our interest in heterometallic 3d-4f systems that possess interesting magnetic behavior^{10,1(e)} we were intrigued if we can utilize oxime ligands to assemble heterometallic compounds. For this purpose, we decided to utilize, 8-quinolinol-2-carboaldoxime (LH₂). The multiple coordination sites on this ligand, two nitrogen atoms (one from ring and another from the oxime) and the two oxygen atoms (the phenolic oxygen and the =N-OH), along with the ability of the ligand to bind both in a chelating and a bridging manner, we reasoned, would allow the synthesis of polynuclear mixed-metal derivatives. To test the efficacy of the ligand LH₂, we investigated its ability to assist the formation of Ni²⁺/Ln³⁺ polynuclear compounds. Accordingly, herein we report the synthesis, structure and magnetism of a family of heterometallic decanuclear complexes, [Ni₈Dy₂(μ₃-OH)₂(L)₈(LH)₂(H₂O)₆](ClO₄)₂·16H₂O (1), [Ni₈Gd₂(μ₃-OH)₂(L)₈(LH)₂(H₂O)₄(MeOH)₂](NO₃)₂·12H₂O (2), [Ni₈Ho₂(μ₃-OH)₂(L)₈(LH)₂(H₂O)₄(MeOH)₂](ClO₄)₂·2MeOH·12H₂O (3) and [Ni₈Tb₂(μ₃-OH)₂(L)₈(LH)₂(MeOH)₄(OMe)₂](ClO₄)₂·2CH₂Cl₂·8H₂O (4). While compounds 1-3 are dicationic, compound 4 is neutral. These complexes, remarkably, possess a unique *S-shaped* architecture. Magnetic studies on 1-4, supported by DFT analysis of the magnetic behavior of 2, reveal that in these compounds the predominantly anti-ferromagnetic behavior observed at low temperatures

can be rationalized based on Ni^{II}-Ni^{II} anti-ferromagnetic interactions and weak Gd^{III}-Ni^{II} ferromagnetic interactions.

EXPERIMENTAL SECTION

Reagents and General Procedures

Solvents and other general reagents used in this work were purified according to standard procedures.¹¹The following chemicals were used as obtained. Ni(ClO₄)₂·6H₂O (Alfa Aesar, India), Dy(NO₃)₃·5H₂O, Gd(NO₃)₃·6H₂O, Ho(NO₃)₃·5H₂O, Tb(NO₃)₃·5H₂O, SeO₂, 2-methyl-8-quinolinol (Aldrich, USA), hydroxylamine hydrochloride (Merck, India). 8-Hydroxy-2-quinolinecarboxaldehyde was prepared by adapting a literature method.¹²

Cautions! Reactions of perchlorate salts of metal complexes with organic ligands are potentially explosive. Only a small amount of material should be prepared, and it should be handled with care.

Instrumentation

Melting points were measured using a JSGW apparatus and are uncorrected. Elemental analyses were carried out by using a Thermo quest CE instrument model EA/110 CHNS-O elemental analyzer. ¹H NMR was recorded on a JEOL-JNM LAMBDA 400 model NMR spectrometer in CDCl₃ solutions. The chemical shifts are referenced with respect to SiMe₄. IR spectra were recorded as KBr pellets on a Bruker Vector 22 FT IR spectrophotometer operating from 400 to 4000 cm⁻¹.

Variable-temperature (2.0–300 K) direct current (dc) magnetic susceptibility measurements for **1-4** under an applied field of 100 ($T < 20$ K) and 1000 G ($T \geq 20$ K), and variable field (0–5.0 T)

magnetization measurements at low temperatures at 2.0 K were carried out with a Quantum Design SQUID magnetometer. The magnetic susceptibility data was corrected for the diamagnetism of the constituent atoms and the sample holder. Dc magnetic measurements were carried out by powdering and restraining the sample in order to prevent any displacement due to its magnetic anisotropy. Theoretical calculations were performed through the Gaussian09 package using the B3LYP functional and the quadratic convergence approach.^{13,14,15,16} Details about the modeling of the data can be found in the ESI.

Synthesis

8-Hydroxyquinoline-2-carbaldehyde

The following procedure has been adapted and modified from a previously published synthetic method.¹² In a two necked round-bottomed flask, freshly sublimed selenium dioxide (6.66 gm, 60 mmol) was taken in 150 ml of dioxane at 60 °C and to it 2-methylquinolin-8-ol (5.2 g, 30 mmol) dissolved in dioxane was added drop wise over a period of 2.5 hour and refluxed at 95 °C for 24 h. The reaction mixture was cooled and filtered through celite; dioxane was removed from the filtrate under reduced pressure. The residue obtained was purified by column chromatography using silicagel 100-200 mesh and 5-10 % ethylacetate-*n*-hexane as the eluent to give the light yellowish compound, 8-hydroxyquinoline-2-carbaldehyde. Yield 4.15 g (80%). MP.: 90 °C. Analysis. Calcd for C₁₀H₇NO₂: C, 69.36; H, 4.07; N, 8.09. Found: C 69.14, H, 4.17; N, 8.24 NMR (CDCl₃) [δ (ppm)]: 7.28 (d, 1H), 7.42 (d, 1H), 7.61 (t, 1H), 8.04 (d, 1H), 8.31(d, 1H), 10.20 (s, 1H). ESI-MS (*m/z*): 174.06 (M+H).

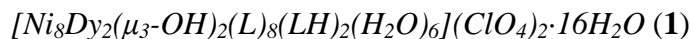
Preparation of 8-hydroxyquinoline-2-carbaldehyde oxime (LH₂)

The synthesis of LH₂ was carried out by adapting a patent procedure known in literature.¹⁷ To a ethanolic solution of 8-hydroxyquinoline-2-carbaldehyde (4.15 g, 24 mmol) was added solid

NH₂OH·HCl (2.00 g, 28.8 mmol) at room temperature and followed by anhydrous CH₃COONa (2.36 g, 28.8 mmol) and refluxed for 12 h. The reaction mixture was allowed to cool to room temperature and filtered. The filtrate was stripped off its solvent in vacuum. Then, to the white residue, dry CHCl₃ was added and the mixture was sonicated for 10 min and filtered. Subsequently, the filtrate was evaporated under reduced pressure affording an opaque white solid, 8-hydroxyquinoline-2-carbaldehyde oxime. Yield 4.64 g (90%). Mp: 120 °C. Anal. Calcd for C₁₀H₈N₂O₂: C, 63.82; H, 4.28; N, 14.89. Found: C, 63.64; H, 4.22; N, 14.95. ¹H NMR (CDCl₃) [δ(ppm)]: NMR (CDCl₃) [δ(ppm)]: 7.20 (d, 1H), 7.33 (d, 1H), 7.47 (t, 1H), 7.90 (d, 1H), 8.15(d, 1H), 8.38 (s, 1H).ESI-MS(*m/z*): 189.06 (M+H).

General Procedure for the Synthesis of Metal Complexes, 1-4

All the complexes (**1-4**), were synthesized by a common procedure. 8-Hydroxyquinoline-2-carbaldehyde oxime (**LH₂**) (1 equivalent) was dissolved in 25 mL of MeOH affording a colorless solution. To this colorless solution Ni(ClO₄)₂·6H₂O (1 eq.) was added in portions affording a light yellowish colored solution which was stirred for 30 min. At this stage, Ln(NO₃)₃·xH₂O (for complex **1**, Ln = Dy and x = 5; **2**, Ln = Gd and x = 6; **3**, Ln = Ho and x = 5; **4**, Ln = Tb and x = 5 respectively) was added and the reaction mixture was stirred for another 15 min. At this point, NEt₃ was added very slowly to the reaction mixture (2 equivalents, neat) affording a straw-colored solution. The reaction mixture was stirred for another 2 h and its volume reduced to 10 mL at 35 °C. To this, was added acetonitrile and dichloromethane (total volume ratio 4:2:1) and filtered. The filtrate was kept for crystallization under slow evaporation conditions. After 15 days, a deep green crystalline material suitable for X-ray analysis was isolated. The quantity of the reactants used in each reaction and the characterization data of the compounds are given below.



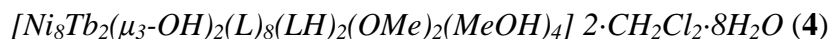
Ni(ClO₄)₂·6H₂O (78 mg, 0.212mmol), Dy(NO₃)₃·5H₂O (46.5 mg, 0.106 mmol), LH₂ (40 mg, 0.212 mmol) and Et₃N (43 mg, 0.424 mmol). Yield: 44 mg, 50% (based on Ni). Mp: >280⁰C. IR (KBr, v/cm⁻¹): 3405 (m, br), 3052 (m, br), 1594 (s), 1513 (s) 1451 (s), 1308 (s), 980 (s), 521(s), 491 (s). Anal.Calcd for C₁₀₀H₁₀₈Cl₂Dy₂N₂₀Ni₈O₅₂: C, 36.56; H, 3.31; N, 8.53; Found: C, 36.32; H, 3.37; N, 8.68.



Ni(ClO₄)₂·6H₂O (78 mg, 0.212 mmol), Gd(NO₃)₃·6H₂O (48.0 mg, 0.106 mmol), LH₂ (40 mg, 0.212mmol) and Et₃N (43mg, 0.424 mmol). Yield: 42 mg, 50% (based on Gd). Mp: >280⁰C. IR (KBr, v/cm⁻¹): 3412 (m, br), 3031 (m, br), 1632 (s), 1592 (s) 1515 (s), 1453 (m) 1312 (s), 780(s), 530(s). Anal. Calcd for C₁₀₂H₁₀₄Gd₂N₂₂Ni₈O₄₆: C, 38.79; H, 3.32; N, 9.76; Found: C, 38.60; H, 3.34; N, 9.67.



Ni(ClO₄)₂·6H₂O (78 mg, 0.212 mmol), Ho(NO₃)₃·5H₂O (47.0 mg, 0.106 mmol), LH₂ (40 mg, 0.212 mmol) and Et₃N (43 mg, 0.424 mmol). Yield: 44 mg, 50% (based on Ho). Mp: >280⁰C. IR (KBr, v/cm⁻¹): 3398 (m, br), 3054 (m, br), 2924 (s), 1594 (s) 1513 (m.), 1451 (m) 1333 (s), 1265(s), 1107 (s), 980 (s), 836 (s), 752 (s), 521 (s), 491 (s). Anal. Calcd for C₁₀₄H₁₁₂Cl₂Ho₂N₂₀Ni₈O₅₀: C, 37.71; H, 3.41; N, 8.46; Found: C, 37.85; H, 3.43; N, 8.54.



Ni(ClO₄)₂·6H₂O (78 mg, 0. 212 mmol), Tb(NO₃)₃·5H₂O (46.0 mg, 0.106 mmol), LH₂ (40 mg, 0.212 mmol) and Et₃N (43 mg, 0.424 mmol). Yield: 42 mg, 50% (based on Tb). Mp: >280⁰C. IR (KBr, v/cm⁻¹): 3300 (m, br), 3059 (m, br), 1652 (s), 1517 (s), (s), 1313 (s) 1107 (s), 840(s), 752

(s), 624 (s). Anal. Calcd for $C_{108}H_{106}Cl_4N_{20}Ni_8O_{36}Tb_2$: C, 40.67; H, 3.35; N, 8.78; Found: C, 40.63; H, 3.28; N, 8.97.

X-ray crystallography

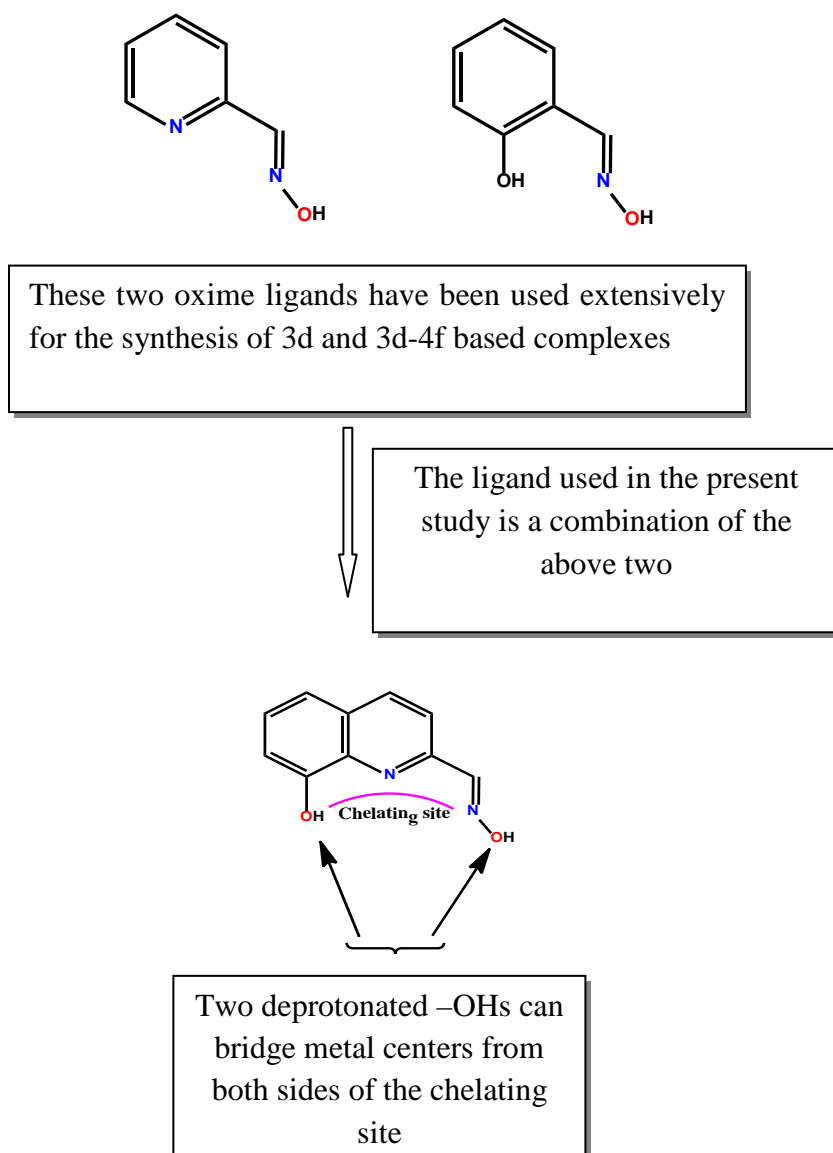
A SMART CCD diffractometer (MoK α radiation, $\lambda = 0.71073 \text{ \AA}$) has been used to collect X-ray data. Complete hemispheres of data were collected using ω -scans (0.3° , up to 20 seconds/frame). SAINT+¹⁸ has been used to obtain integrated intensities and SADABS^{18b} has been used for the absorption correction of this integrated intensity. For structural solution and refinement SHELXTL-package has been used.^{18c} The structures were solved by direct methods and completed by iterative cycles of DF syntheses and full-matrix least-squares refinement against F^2 .^{18d} All the non-hydrogen atoms were refined with anisotropic displacement parameters. All the hydrogen atoms on carbon, nitrogen and oxygen frameworks were included in the final stages of the refinement and were refined with a typical riding model. Some hydrogen atoms on the solvent molecules could not be located; these were included in the molecular formula directly. In addition, the high R1 and wR2 factor of complex (**1** and **4**) might be due to the weak high-angle diffractions. The crystallographic figures have been generated using Diamond 3 software.¹⁹ The crystal data and the cell parameters for compounds **1–4** are summarized in Table 1.

Table 1. Crystal data and structure refinement parameters of 1-4.

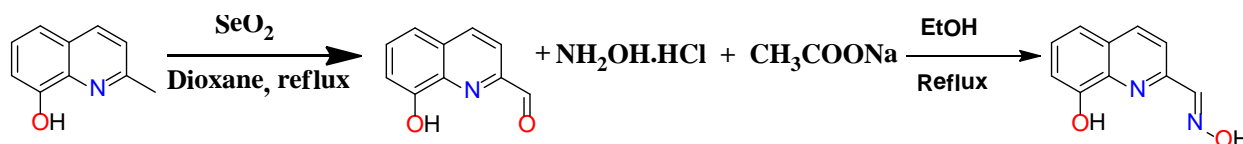
Compound	1	2	3	4
Formula (calculated/modeled)	C ₁₀₀ H ₇₂ Cl ₂ Dy ₂ N ₂₀ Ni ₈ O ₅₂	C ₁₀₂ H ₇₄ Gd ₂ N ₂₂ Ni ₈ O ₄₆	C ₁₀₄ H ₈₈ Cl ₂ Ho ₂ N ₂₀ Ni ₈ O ₅₀	C ₁₀₈ H ₁₀₆ Cl ₄ N ₂₀ Ni ₈ O ₃₆ Tb ₂
Mw/g	3251.20	3127.86	3288.23	3165.12
crystal system	Monoclinic	Monoclinic	Monoclinic	Monoclinic
Cell measurement temperature (K)	100	100	100	100
space group	<i>P</i> 2 ₁ / <i>c</i>	<i>P</i> 2 ₁ / <i>c</i>	<i>P</i> 2 ₁ / <i>c</i>	<i>P</i> 2 ₁ / <i>c</i>
<i>a</i> /Å	18.104(5)	18.148(5)	18.181(5)	18.595(5)
<i>b</i> /Å	21.575(5)	21.542(6)	21.581(5)	21.805(5)
<i>c</i> /Å	17.072(5)	17.094(5)	17.132(4)	17.277(5)
β (°)	115.356(5)	114.989(5)	114.918(5)	116.236(5)
<i>V</i> /Å ³	6026(3)	6057(3)	6096(3)	6284(3)
<i>Z</i>	2	2	2	2
ρ_c /g cm ⁻³	1.792	1.715	1.791	1.673
μ /mm ⁻¹	2.589	2.387	2.631	2.448
<i>F</i> (000)	3236	3120	3288	3160
cryst size (mm ³)	0.015 x 0.012 x 0.01	0.015 x 0.012 x 0.01	0.015 x 0.012 x 0.01	0.015 x 0.012 x 0.010
θ range (deg)	1.89 to 25.50	4.13 to 25.03	4.12 to 25.03	4.11 to 25.03
limiting indices	-20 ≤ <i>h</i> ≤ 21 -25 ≤ <i>k</i> ≤ 26 -20 ≤ <i>l</i> ≤ 12	-21 ≤ <i>h</i> ≤ 21 -25 ≤ <i>k</i> ≤ 23 -12 ≤ <i>l</i> ≤ 20	-17 ≤ <i>h</i> ≤ 21 -25 ≤ <i>k</i> ≤ 25 -20 ≤ <i>l</i> ≤ 13	-22 ≤ <i>h</i> ≤ 17 -25 ≤ <i>k</i> ≤ 25 -20 ≤ <i>l</i> ≤ 20
reflns collected	31306	30239	31486	31619
indreflns	11114 [R(int) = 0.1331]	10614 [R(int) = 0.1604]	10733 [R(int) = 0.1471]	11049 [R(int) = 0.0720]
completeness to θ (%)	99.0	99.1	99.5	99.4
refinement method	Full-matrix least-squares on <i>F</i> ²	Full-matrix least-squares on <i>F</i> ²	Full-matrix least-squares on <i>F</i> ²	Full-matrix least-squares on <i>F</i> ²
data/restraints/params	11114 / 52 / 796	10614 / 25 / 784	10733 / 60 / 806	11049 / 30 / 793
goodness-of-fit on <i>F</i> ²	1.036	0.973	0.967	1.090
Final R indices [<i>I</i> > 2 θ (<i>I</i>)]	<i>R</i> 1 = 0.1124 <i>w</i> <i>R</i> 2 = 0.2641	<i>R</i> 1 = 0.0931 <i>w</i> <i>R</i> 2 = 0.2138	<i>R</i> 1 = 0.0852 <i>w</i> <i>R</i> 2 = 0.1804	<i>R</i> 1 = 0.1048 <i>w</i> <i>R</i> 2 = 0.2642
R indices (all data)	<i>R</i> 1 = 0.2186 <i>w</i> <i>R</i> 2 = 0.3278	<i>R</i> 1 = 0.2288 <i>w</i> <i>R</i> 2 = 0.2826	<i>R</i> 1 = 0.2002 <i>w</i> <i>R</i> 2 = 0.2362	<i>R</i> 1 = 0.1480 <i>w</i> <i>R</i> 2 = 0.2915
largest diff. peak and hole(e · Å ⁻³)	2.570 and -1.732	1.431 and -1.298	1.441 and -1.213	2.267 and -2.057

RESULTS AND DISCUSSION

Synthetic aspects

**Chart 1:** Design aspects of the ligand **LH₂**

The ligand LH₂ was prepared as shown in Scheme 1. Accordingly, first, 8-hydroxyquinoline-2-carbaldehyde was prepared by an oxidation of 2-methylquinolin-8-ol. This was followed by a condensation reaction with hydroxylamine hydrochloride affording LH₂ in good yields (see experimental section; Scheme 1). The reaction of LH₂ with a Ni(II) salt, followed by a Ln(III) salt in the presence of triethylamine afforded the heterometallic decanuclear complexes, [Ni₈Dy₂(μ₃-OH)₂(L)₈(LH)₂(H₂O)₆](ClO₄)₂·16H₂O (1), [Ni₈Gd₂(μ₃-OH)₂(L)₈(LH)₂(H₂O)₄(MeOH)₂](NO₃)₂·12H₂O (2), [Ni₈Ho₂(μ₃-OH)₂(L)₈(LH)₂(H₂O)₄(MeOH)₂](ClO₄)₂·2MeOH·12H₂O (3) and [Ni₈Tb₂(μ₃-OH)₂(L)₈(LH)₂(MeOH)₄(OMe)₂]·2CH₂Cl₂·8H₂O (4) in good yields (>50 %, see experimental section). Previously, the only known instance of assembling a mixed Ni(II)-Ln(III) system [a Ni₈-Dy₈ system] from an oxime ligand, involved the ligand 2-pyridyl aldoxime.²⁰



Scheme 1: Synthesis of ligand LH₂

X-ray crystal structures of 1-4

Molecular structures of **1-4** have been established by single crystal X-ray diffraction analysis. All the complexes crystallize in the monoclinic space group $P2_1/c$ with $Z = 2$. The asymmetric unit of all these complexes contains one half of the molecule. Complexes **1-3** are dicationic and have two bridging μ₃-OH, eight dianionic ligands, two monoanionic ligands in the structure. In contrast, **4** is neutral and possesses two [OMe]⁻ ligands, two bridging hydroxo μ₃-OH, eight dianionic ligands, [L]²⁻ and two monoanionic ligands, [LH]⁻. BVS calculations were carried out to confirm the nature of the hydroxide ligand present in **1-4** (ESI Table S1). While compounds **1**

and **3** have two perchlorate counter anions, **2** has two nitrate counter anions. All the complexes possess six solvent molecules within the coordination sphere of the metal ions (**1**, six H₂O; **2**, four H₂O and two MeOH; **3**, four H₂O and two MeOH; **4**, four MeOH and two MeO⁻). Further, these complexes contain several non-coordinating solvent molecules as solvents of crystallization (**1**, 16 H₂O; **2**, 12 H₂O; **3**, 2 MeOH and 12 H₂O; **4**, two CH₂Cl₂ and 8 H₂O).

The broad structural features of **1-4** are quite similar. Accordingly, the structure of **1** will be described in detail as a representative example to illustrate the common structural features present in these four compounds. The molecular structure of **1** is given in Figure 1; the decanuclear core is shown in Figure 2. The mode of coordination of the various ligands in **1** is summarized in Figure 3. The structural diagrams of **2-4** are given in the ESI. Selected bond distances found in **1** are summarized in the caption of Figure 4. The other bond parameters of **1-4** are given in the ESI.

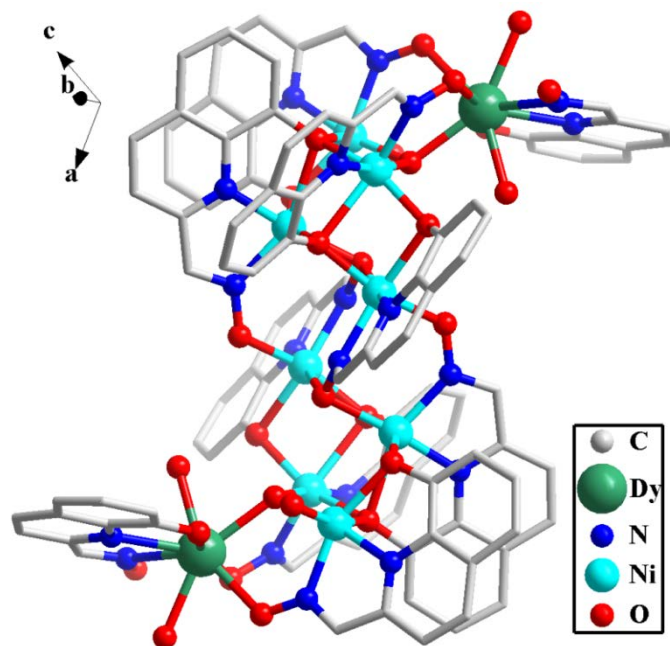


Figure 1. Cationic part of the compound $[\text{Ni}_8\text{Dy}_2(\text{OH})_2\text{L}_8(\text{LH})_2]^{2+}$ (**1**). Hydrogen atoms, perchlorate anions and solvent molecules have been omitted for clarity.

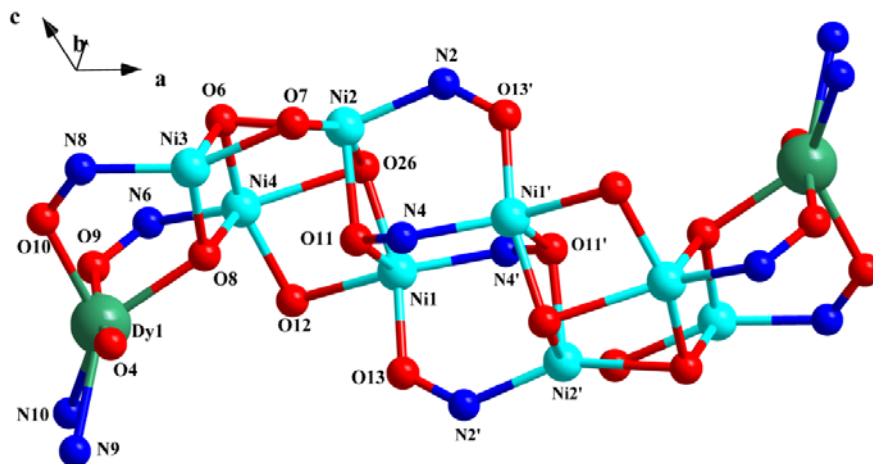


Figure 2. The decametallc core of **1**. Carbon and hydrogen atoms, perchlorate anions and solvent molecules have been omitted for clarity.

Compound **1** possesses a *S-shaped* architecture among mixed-metal assemblies and comprises a long chain of metal ions bound to each other. The eight Ni(II) and two Dy(III) ions of the multimetallic ensemble are held together by two μ_3 -OH, eight dianionic (L^{2-}) and two monoanionic oxime ligands (LH^-) (see Figure 3 for the coordination behavior of various ligands). The *S-shaped* molecular wire has at its two ends the Dy(III) caps. The Dy-Dy distance is 13.518 (1) Å while the end-to-end H-H distance is 21.240 (4) Å indicating the nanometric size of the molecular wire.

Every metal ion in **1** is bound by one multi-topic oxime ligand in a chelating fashion. Thus, each Dy(III) is bound by a $[LH^-]$ ligand and each Ni(II) is coordinated by a $[L]^{2-}$ ligand (Figure 3). This coordination behavior leads to the formation of two 5-membered chelating rings around each metal ion. While the N-OH is free in the ligands attached to Dy(III) while it is bound in the ligands attached to Ni(II). The formation of the entire metal ensemble could be understood in the following manner. The terminal Dy(III) (Dy1) and two Ni(II) centres (Ni3 and Ni4) are attached to each other by a μ_3 -OH affording a Dy-Ni₂ motif. The nickel centres of this unit are connected to two other nickel ions (Ni1 and Ni2) by the phenolate oxygen atoms generating the Dy-Ni₄ motif. The inter-connection of two such centrosymmetrically related motifs by the oximate group $[N-O]^-$ groups affords the molecular multi-metal assembly. As a result of this cumulative coordination action each metal ion is part of several ring systems which is another unique structural feature of this family of heterometallic compounds: [around Dy1, (a) Dy1-N10-C50-C50-C49-N9 (b) Dy1-N9-C46-C41-O4 (c) Dy1-O10-N8-Ni3-O8 (d) Dy1-O8-Ni4-N6-O9], [around Ni3, (a) Ni3-N8-C40-C39-N7 (b) Ni3-N7-C36-C31-O7 (c) Ni3-O8-Dy1-O10-N8], [around Ni1 (a) Ni1-N4-C11-C12-N3 (b) Ni1-N3-C16-C17-O12 (c) Ni1-O26-Ni4-O12], [around Ni4 (a) Ni4-O12-Ni1-O26 (b) Ni4-N6-C30-C29-N5 (c) Ni4-N5-C26-C21-O26 (d) Ni4-O8-Dy1-

O9-N26],[around Ni2 (e) Ni4-O8-Ni3-O7-Ni2-O26], [connecting rings between two asymmetric units (a) Ni1'-N4-O11-Ni2-O13' (b) Ni2'-O11'-N4'-Ni1-O13-N2' (c) Ni1'-O11'-N4'-Ni1-O11-N4] (Figure 2).

Compound **1** contains one type of Dy(III) which is eight-coordinate (6O, 2N) in an approximate dodecahedral coordination environment (Figure 4a). On the other hand there are four types of Ni(II) each of which is six-coordinate (4O, 2N) in a distorted octahedral geometry (Figure 4b)

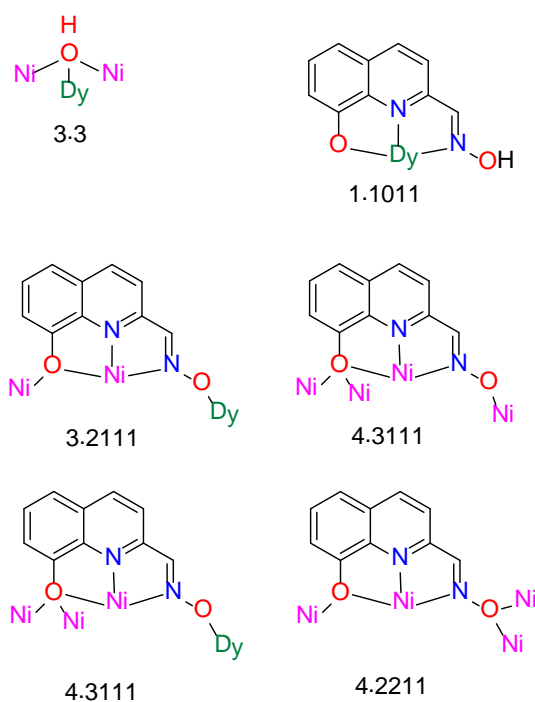


Figure 3. Binding mode of the ligand LH₂ in its [LH]⁻ and [L]²⁻ forms. The coordination notation is according to the one proposed by Harris and co-workers²¹

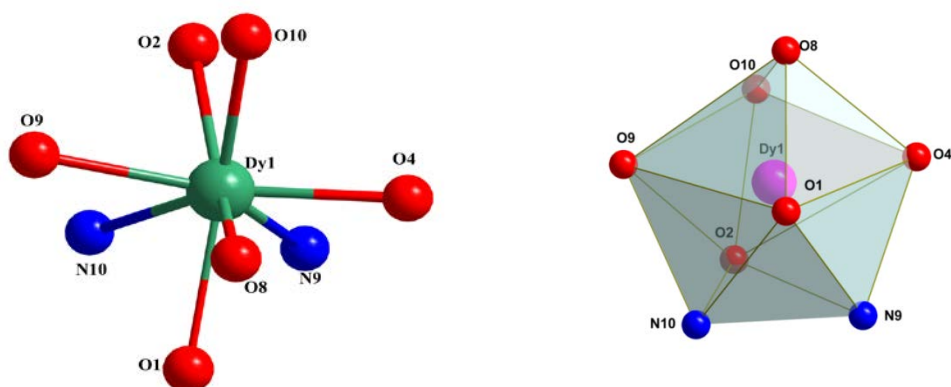


Figure 4a. A dodecahedral coordination environment around the Dy^{3+} ion in **1**. Selected bond distances around Dy^{3+} (Å) : Dy1-O1, 2.388(6); Dy1-O2, 2.389(5); Dy1-O4, 2.264(4); Dy1-O8, 2.353(4); Dy1-O9, 2.347(4); Dy1-O10, 2.336(5); Dy1-N9, 2.481(9); Dy1-N10, 2.574(5)

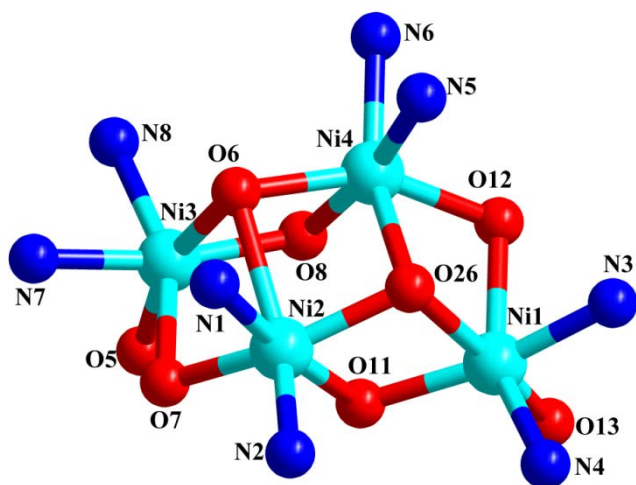


Figure 4b. The distorted octahedral geometry around the various Ni^{2+} ions in **1**.

Selected bond distances around Ni^{2+} (in Å) : Ni1-N3, 1.962(6); Ni1-N4, 2.052(6); Ni1-O11, 2.028(5); Ni1-O12, 2.260(5); Ni1-O13, 1.990(4); Ni1-O26, 2.064(5); Ni2-N1, 1.980(6); Ni2-N2, 2.057(6); Ni2-O6, 2.426(6); Ni2-O7, 1.971(5); Ni2-O11, 2.127(4); Ni2-O26, 1.991(4);

Ni3-N7, 2.001(3); Ni3-N8, 2.065(8); Ni3-O5, 2.085(4); Ni3-O6, 2.081(4); Ni3-O7, 2.197(5); Ni3-O8, 2.040(4); Ni4-N5, 2.026(6); Ni4-N6, 2.045(7); Ni4-O6, 2.037(4); Ni4-O8, 2.095(4), Ni4-O12, 2.027(5); Ni4-O26, 2.395(5).

Magnetic Properties. The direct current (dc) magnetic properties of **1–4** in the form of the $\chi_M T$ versus T plots (χ_M being the dc molar magnetic susceptibilities per $\text{Ni}^{\text{II}}_8\text{Ln}_2^{\text{III}}$ unit), have been investigated in the temperature range 2.0–300 K (Figure 5). The $\chi_M T$ values of 36.04 (**1**), 24.70 (**2**), 36.79 (**3**) and 29.10 $\text{cm}^3 \text{mol}^{-1} \text{K}$ (**4**) at room temperature are close to those expected for the sum of eight non-interacting octahedral high-spin Ni^{II} ions ($\chi_M T_{\text{Ni}} \approx 1.10 \text{ cm}^3 \text{mol}^{-1} \text{K}$) and the corresponding lanthanide ion; **1**: Dy^{III} ($\chi_M T_{\text{Dy}} = 14.15 \text{ cm}^3 \text{mol}^{-1} \text{K}$ with $S = 5/2$, $L = 5$, ${}^6H_{15/2}$, $g = 4/3$), **2**: Gd^{III} ($\chi_M T_{\text{Gd}} = 7.88 \text{ cm}^3 \text{mol}^{-1} \text{K}$ with $S = 7/2$, $L = 0$, ${}^8S_{7/2}$, $g = 2$), **3**: Ho^{III} ($\chi_M T_{\text{Ho}} = 14.05 \text{ cm}^3 \text{mol}^{-1} \text{K}$ with $S = 2$, $L = 6$, 5I_8 , $g = 5/4$) and **4**: Tb^{III} ($\chi_M T_{\text{Tb}} = 11.81 \text{ cm}^3 \text{mol}^{-1} \text{K}$ with $S = 3$, $L = 3$, 7F_6 , $g = 3/2$). This behavior indicates that the magnetic interactions between neighboring metal ions are negligible at room temperature.

The lack of orbital contribution to the magnetic moment in gadolinium(III) ions makes the magnetic properties of compound **2** the easiest ones to be analysed (Figure 5). Upon cooling, the $\chi_M T$ value for **2** decreases very smoothly down to *ca.* 100 K and then decreases faster, probably due to $\text{Ni}^{\text{II}}\text{-Ni}^{\text{II}}$ antiferromagnetic interactions, to reach a minimum with a $\chi_M T$ value of 21.44 $\text{cm}^3 \text{mol}^{-1} \text{K}$ at 9 K (see inset of Figure 5). Finally, $\chi_M T$ slightly increases to reach a value of 22.45 $\text{cm}^3 \text{mol}^{-1} \text{K}$ at 2 K suggesting the presence of $\text{Gd}^{\text{III}}\text{-Ni}^{\text{II}}$ ferromagnetic interactions. The nature of the magnetic interactions of **2** is discussed in detail in the Theoretical Calculations section (below). We have also discussed the fit of the $\chi_M T$ vs. T curve in this section for the sake of clarity.

The magnetic properties of **1**, **3** and **4** are more complicated²² because of the intervening first-order angular momentum and crystal field effects for the Dy^{III} (**1**), Ho^{III} (**3**) and Tb^{III} (**4**) ions. Upon cooling, $\chi_M T$ for all of them decreases gradually to reach values of 24.40, 13.50 and 16.64 cm³ mol⁻¹ K at 2 K, respectively, suggesting antiferromagnetic interactions between the nickel(II) ions and/or the first-order angular momentum and crystal field effects of the lanthanide ions. Figure 7 shows the magnetization curves for **1-4**. The saturation values tend in all cases to lower values to those expected for the isolated ions due, mainly, to the crystal field effects on the lanthanide ions, but also suggesting that antiferromagnetic interactions dominate in all the compounds. Although AC magnetic measurements were carried out, no single-molecule magnet behavior was observed for any compound.

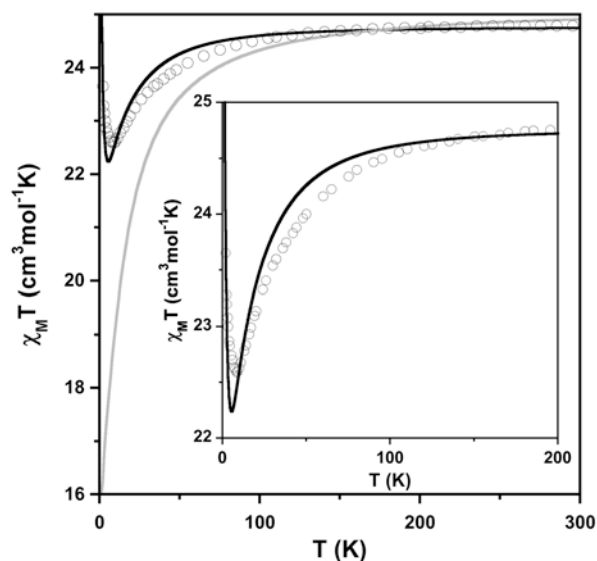


Figure 5. Experimental (circles) and theoretical (lines) χT vs T curves for **2**. The theoretical curves were obtained from a diagonalization of the energy matrix built from the J values provided by the DF study (in grey) or from the J values found in the fitting (in black). The inset shows the minimum of $\chi_M T$ for **2** in detail.

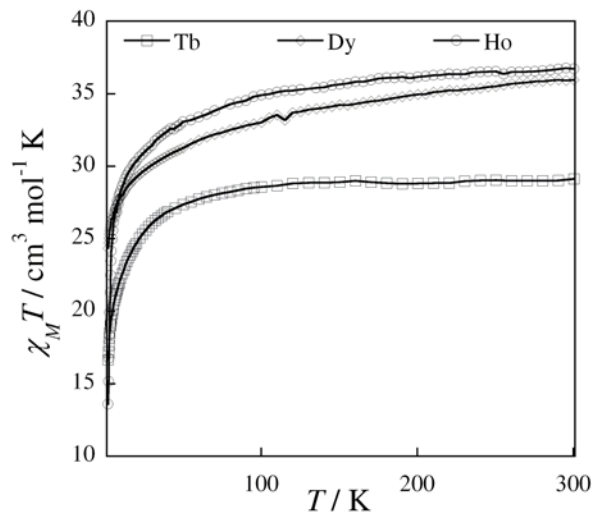


Figure 6. Temperature dependence of $\chi_M T$ for **1** (\diamond), **3** (\circ) and **4** (\square).

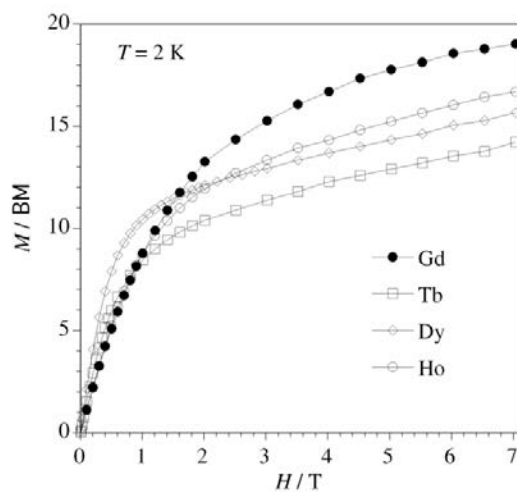
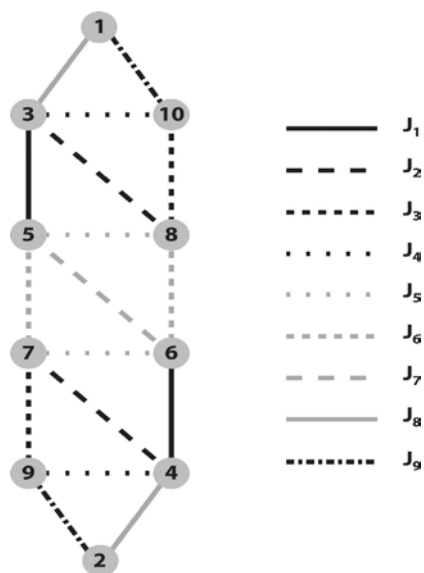


Figure 7. Field dependence of M for **1** (\diamond), **2** (\bullet), **3** (\circ) and **4** (\square).

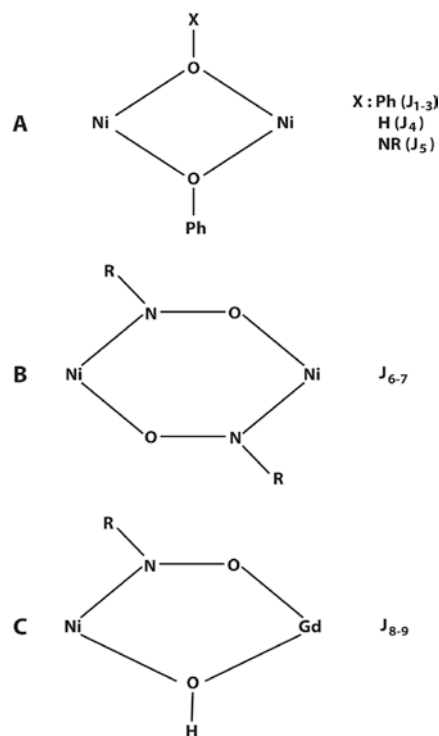
Theoretical Calculations. In order to analyze the magnetic behavior of compound **2** we performed electronic structure calculations based on Density Functional Theory (DFT) for **2** following the method described in the computational details paragraph (see ESI).

Compound **2** is constructed from a complex Ni_8 core built from two symmetric Ni_4 units. Two additional Gd^{III} ions lie on either side of this central structure. Scheme **2** shows that nine

different magnetic couplings can be proposed from the geometrical parameters. Knowing the magnitude and nature of these magnetic couplings should allow identifying the electronic features of the spin ground state and helping to interpret the experimental magnetic behavior. It is for this purpose that electronic structure calculations based on *density functional theory* (DFT) were carried out.



Scheme 2. Scheme of the magnetic exchange interactions present in complex **2**. The Gd³⁺ (1 and 2) and Ni²⁺ ions (3-10) are represented as grey circles.



Scheme 3. Magnetic couplings present in **2** (see text).

Analyzing the possible pathways involved in the magnetic coupling between the paramagnetic centers it is possible to visualize nine different magnetic couplings that can be organized in three groups. In group **A** (Scheme 3), the two Ni^{II} ions are connected through two $\mu\text{-O}$ ligands; these oxygen atoms, however, can be from more than one kind of ligands (oxime, hydroxo or phenoxo groups). Group **B** brings together the magnetic couplings that link two Ni^{II} ions via NO pathways from the oxime groups. Finally, the $\text{Ni}^{\text{II}}\text{-Gd}^{\text{III}}$ magnetic couplings in which NO-oxime and O-hydroxo groups act as magnetic pathways are grouped in **C**. Due to the development and availability of only a few basis sets for the gadolinium atoms, together with the need for the inclusion of relativistic effects inherent to this heavy atom and the fact the ground spin topology is governed by the stronger Ni-Ni magnetic interactions, a preliminary study was done just on the Ni_8 core. To facilitate this, Gd^{III} ions were replaced by relativistic La^{III} and non-relativistic Sc^{III}

ions, which allowed minimizing electronic effects associated with the molecular cutting process. Calculated spin configurations are shown in Table 2, which also shows the relative energies as a function of the J_i magnetic coupling constants where a spin configuration with all local spin moments that are parallel-organized (HS, maximum S value). The spin Hamiltonian used to build this table is as follows: $H = -J_1(S_3S_5 + S_4S_6) - J_2(S_3S_8 + S_4S_7) - J_3(S_7S_9 + S_8S_{10}) - J_4(S_3S_{10} + S_4S_9) - J_5(S_5S_8 + S_6S_7) - J_6(S_5S_7 + S_6S_8) - J_7S_5S_6 - J_8(S_1S_3 + S_2S_4) - J_9(S_1S_{10} + S_2S_9)$.

Although only a limited number of the spin configurations – beyond the HS reference configuration – equal to the different magnetic coupling constants are needed to solve the set of equations that link these magnetic coupling constants and the energy of each state, a larger number of spin configurations were calculated to check the quality and validity of the results (Tables 2 and 3). The values of the calculated magnetic coupling constants together with the more relevant structural parameters are given in Table 4. In order to show that the relativistic or non-relativistic feature of the M^{III} ions do not have any effect on the calculated energies, Sc and La models were employed giving similar J_i values than those found for Gd^{III} ions (Table 3). Some conclusions can be inferred from these results. (1) Similar ferromagnetic couplings were found for J_{1-3} , which belong to the A interaction group. The differences in the J values were associated to the small geometrical differences in the Ni_2O_2 core. Thus, it seems that smaller NiONi angles lead to stronger ferromagnetic couplings; but, mainly, the weaker couplings are observed when the Ni_2O_2 core is less distorted and closer to the planar conformation. However, the proposed nature of the J_4 and J_5 couplings, which are also in the A interaction group, was clearly antiferromagnetic which is tied to larger NiONi angles (around 102°) and to a quasi-planar conformation of the Ni_2O_2 core (dihedral angles around 17°), without excluding the possibility of the electronic effects by the presence of hydroxo or oxime instead of phenoxo

pathways. (2) Despite the dissimilar degree of distortion on the Ni₂O₂N₂ core of the magnetic couplings included in the **B** interaction group that moves this unit away from the planarity, close antiferromagnetic couplings were proposed, probably due to the fact that the structural change was not large enough. The conformation of the Ni₂O₂N₂ core suggested strong overlapping between magnetic orbitals that firmly contributed to an antiferromagnetic coupling. (3) Finally, weaker ferromagnetic couplings were predicted for the Gd^{III}-Ni^{II} magnetic couplings (J_8 and J_9). This is consistent with that expected for a magnetic interaction between *d* and *f* orthogonal magnetic orbitals. It may be mentioned that ferromagnetic couplings have been usually found between a Gd^{III} ion and a Cu^{II} or Ni^{II} ion.^{1f,g}

Table 2. Calculated spin configurations and their relative energies as a function of different J_i constants for **2**. The spin configuration used as a reference is that with the maximum multiplicity that is generated from the parallel alignment of all local spin moments of the Gd(III) and Ni(II) ions. Only the centers with an antiparallel (negative) alignment of their spin moment are noted in the label following the notation used in Scheme 2.

Spin conf	S	J_1	J_2	J_3	J_4	J_5	J_6	J_7	J_8	J_9
{5,6}	11	6	0	0	0	6	6	0	0	0
{7,8}	11	0	6	6	0	6	6	0	0	0
{3,4}	11	6	6	0	6	0	0	0	16	0
{9,10}	11	0	0	6	6	0	0	0	0	16
{8,9}	11	0	3	6	3	3	3	0	0	8
{5,6,7,8}	7	6	6	6	0	0	0	0	0	0
{5,6,9,10}	7	6	0	6	6	6	6	0	0	16
{4,6,7,8,9}	5	0	3	3	0	3	3	3	8	8
{4,6,8,9,10}	5	0	3	3	3	6	0	3	8	16
{1,2}	1	0	0	0	0	0	0	0	16	16

{2,4,6,7,9} 0 0 0 0 0 0 6 3 0 0

Table 3. Calculated spin configurations and their relative energies as a function of different J_i constants for model Sc_2Ni_8 and La_2Ni_8 . The spin configuration used as a reference is that with the maximum multiplicity that is generated from the parallel alignment of all local spin moments of the Ni(II) ions. Only the centers with an antiparallel (negative) alignment of their spin moment are noted.

Spin conf	S	J_1	J_2	J_3	J_4	J_5	J_6	J_7
{3,6}	4	6	3	0	3	3	3	3
{4,8}	4	3	6	3	3	3	3	0
{3,4,5}	2	3	6	0	6	3	3	3
{3,4,7}	2	6	3	3	6	3	3	0
{3,5,7}	2	0	6	3	3	6	0	3
{3,5,9}	2	0	3	3	6	3	3	3
{3,6,9}	2	6	3	3	6	3	3	3
{4,6,8,9}	0	0	6	6	0	6	0	3
{4,5,6,10}	0	3	3	3	6	6	6	0
{5,6,7,8}	0	6	3	0	3	3	3	0

Table 4. More relevant structural parameters involved in the different magnetic exchange pathways on **2**, **Sc₂Ni₈** and **La₂Ni₈** models and their J values (in cm^{-1}) estimated from DF calculations (see Text). The different magnetic couplings were associated to different kinds of magnetic pathways as it is shown in Figure 2. α (in degrees) is the NiONi angle, θ (in degrees) is the out-of-plane of the R group of alkoxo or hydroxo groups with regard to the metal core calculated as the ROO angle for Ni_2O_2 cores or as the angle between the OR vector and the Ni_2O plane for a planar core, and τ (in degrees) is the dihedral angle related to a butterfly distortion of the Ni_2O_2 core. A τ value equal to 180 degrees corresponds to a planar conformation of the Ni_2O_2 core.

Pathway	Kind	α	θ	τ	J value		
					Gd ₂ Ni ₆	Sc ₂ Ni ₆	La ₂ Ni ₆
J_1	A	91.3	63.7	149.3	+ 8.7	+ 9.5	+ 9.2
		96.2	72.8				
J_2	A	88.6	67.7	141.4	+ 11.1	+ 11.4	+ 11.9
		92.0	73.1				
J_3	A	87.2	71.6	145.1	+ 11.3	+ 13.6	+ 12.7
		97.3	68.8				
J_4	A	102.7	54.1	176.2	- 11.6	- 9.3	- 10.1
		102.9	17.6				
J_5	A	99.9	49.7	167.0	- 12.9	- 9.2	- 12.6
		103.5	11.6				
J_6	B	---	---	---	- 17.2	- 19.4	- 17.1
J_7	B	---	---	---	- 14.5	- 15.4	- 14.6
J_8	C	110.7	58.6		+ 0.1		
J_9	C	113.7	57.9		+ 0.4		

A theoretical χT vs T curve simulated from the J values obtained from the DF calculations on **2** is shown in Figure 5 (Magnetic Properties section). Although a similar behavior is reproduced, some differences with the experimental data are found. Since the Gd^{III} - Ni^{II} magnetic couplings are much weaker than the Ni^{II} - Ni^{II} ones when comparing the $n_A n_B J$ parameter, where n_A and n_B are the number of unpaired electrons of the interacting centers, the magnetic behavior of **2** was analyzed from the data of the Ni_8 core. Although, it is well-known that in frustrated systems like this, the spin topology of the ground spin state is not so easy to propose, a diagonalization of the energy matrix built from the theoretical J values shown a singlet as the ground state. However, two triplet excited states were placed to 5.3 and 6.0 cm^{-1} and several triplet, quintet and even other singlet excited states were found from 11.2 to 16.9 cm^{-1} . Thus, no longer changes in the J values could change the spin ground state. Even, this set of J values can reproduce the continuous decrease of χT when cooling (Figure 5), the presence of a minimum in χT and its later increase cannot be explained. That is why, in agreement with the DF conclusions, weak ferromagnetic couplings (J_8 and J_9) between Gd^{III} ions and some Ni^{II} ions must be present with a quintet spin ground state for the Ni_8 core. The presence of a continuous increase of the experimental χT product at low temperature indicates that the local magnetic anisotropy for Ni^{II} ions was probably too small to show a detectable effect and thus, it was neglected in our study. On the other hand, the reduced magnetization at several temperatures are usually used to determine the presence of a magnetic anisotropy and, eventually, to estimate their corresponding axial and equatorial parameters (D and E). These curves only overlap when the magnetic anisotropy is zero. However, they could not provide additional information because the presence of excited states very close to the ground state in Ni_8 core (see above) avoided the overlapping of

these curves. This fact became stronger when weak Ni-Gd magnetic interactions were included (see below).

A tentative fit was done simplifying the spin interaction topology shown in Figure 1, and described by the spin Hamiltonian in equation (1), by reduction of the numbers of different magnetic coupling constants, which helped to avoid an overparametrization. Thus, according to the kind of pathways and the J values proposed from DF calculations, J_{1-3} , J_{4-5} , J_6 , J_7 , and J_{8-9} were grouped in J_a , J_b , J_c , J_d , and J_e , respectively. The best fit starting from the DF J values was found with the following values: $g_{Gd} = 2.000$, $g_{Ni} = 2.123$, $J_a = +11.6 \text{ cm}^{-1}$, $J_b = -10.2 \text{ cm}^{-1}$, $J_c = -10.9 \text{ cm}^{-1}$, $J_d = -17.9 \text{ cm}^{-1}$ and $J_e = +0.44 \text{ cm}^{-1}$. The agreement factor, defined as $F = \sum[\chi_{obs}^T - \chi_{calc}^T]^2 / \sum[\chi_{obs}^T]^2$, was 4×10^{-4} . The found g and J values are reasonable and the last ones are also similar to those proposed from DF calculations. Although a good qualitative agreement between simulated and experimental curves was found, there were qualitative discrepancies that can be explained by the simplification of the model and the non-inclusion of the magnetic anisotropy of the Ni^{II} ions. These J values led to a $S = 9$ ground state with 38 excited states from $S = 15$ to $S = 0$ in an energy gap equal to 3 cm^{-1} , which prevent any attempt to analyze magnetization data.

Summary

We have utilized an oxime-based multi-site coordination ligand to prepare heterometallic decanuclear 3d/4f complexes $[Ni_8Dy_2(\mu_3-OH)_2(L)_8(LH)_2(H_2O)_6](ClO_4)_2 \cdot 16H_2O$ (**1**), $[Ni_8Gd_2(\mu_3-OH)_2(L)_8(LH)_2(H_2O)_4(MeOH)_2](NO_3)_2 \cdot 12H_2O$ (**2**), $[Ni_8Ho_2(\mu_3-OH)_2(L)_8(LH)_2(H_2O)_4(MeOH)_2](ClO_4)_2 \cdot 2MeOH \cdot 12H_2O$ (**3**) and $[Ni_8Tb_2(\mu_3-OH)_2(L)_8(LH)_2(MeOH)_4(OMe)_2] \cdot 2CH_2Cl_2 \cdot 8H_2O$ (**4**). In addition to the oxime ligand the assembly of the decanuclear ensembles is made possible by bridging hydroxide (**1-4**) ligands.

The molecular structure of these decanuclear complexes reveals an *S*-shaped topology with a central octanuclear Ni^{II} core that is bound on either end with a Ln^{III}. Magnetic studies on these complexes reveal an overall anti-ferromagnetic behavior. Detailed *DF* calculations suggest that the observed magnetic behavior is a cumulative feature that involves a predominant Ni^{II}-Ni^{II} anti-ferromagnetic and weak Gd^{III}-Ni^{II} ferromagnetic interactions.

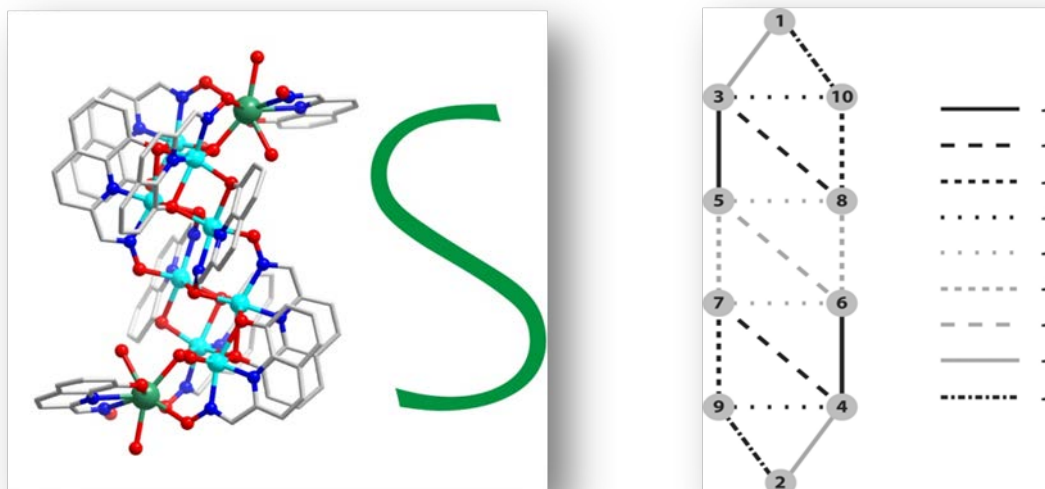
ACKNOWLEDGEMENTS

V.C. thanks the Department of Science and Technology for a J.C. Bose fellowship. S.H., S.D. and A.D. thank the Council of Scientific and Industrial Research, India, for a senior research fellowship. E. P. thanks the Ayuntamiento de Valencia for a contract. This work was also supported by the MICINN (Spain) (Project CTQ2010-15364), the University of Valencia (Project UV-INV-AE11-38904), the Generalitat Valenciana (Spain) (Projects PROMETEO/20.09/108, GV/2012/051 and ISIC/2012/002).

Electronic Supplementary Information (ESI). Crystallographic information files (CIF), CCDC number 986609-986612 for **1-4.**, Tables of bond distance (Å), bond angle (°) and additional figures.

Graphical Abstract

Reaction of the tetradentate Schiff base oxime ligand (**LH**₂) with Ni(ClO₄)₂·6H₂O and Ln(NO₃)₃·xH₂O salts in the presence of the triethylamine as the base, afforded series of S-shape dodecanuclear [Ni₈Ln₂] (Ln= Gd, Tb, Dy, Ho) complexes. Magnetic study of the complexes reveal over all anti-ferromagnetic interactions. Detail theoretical modeling of magnetic property of [Ni₈Gd₂] complex (**2**) shows strong Ni^{II}-Ni^{III} anti-ferromagnetic interaction and weak Ni^{II}-Ln^{III} interaction.



REFERENCES

- ¹ (a) Y.-Z. Zheng, M. Evangelisti and R. E. P. Winpenny, *Chem. Sci.*, 2011, **2**, 99; (b) Y.-Z. Zheng, M. Evangelisti and R. E. P. Winpenny, *Angew. Chem. Int. Ed.*, 2011, **50**, 3692; (c) Y.-Z. Zheng, E. M. Pineda, M. Helliwell and R. E. P. Winpenny, *Chem. Eur. J.*, 2012, **18**, 4161; (d)

Y.-Z. Zheng, M. Evangelisti, F. Tuna and R. E. P. Winpenny, *J. Am. Chem. Soc.*, 2012, **134**, 1057; (e) V. Chandrasekhar, B. M. Pandian, R. Azhakar, J. J. Vittal and R. Clerac, *Inorg. Chem.*, 2007, **46**, 5140; (f) V. Chandrasekhar, B. M. Pandian, R. Boomishankar, A. Steiner, J. J. Vittal, A. Houry and R. Clerac, *Inorg. Chem.*, 2008, **47**, 4918; (g) M. A. Palacios, A. J. Mota, J. E. Perea-Buceta, F. J. White, E. K. Brechin and E. Colacio, *Inorg. Chem.*, 2010, **49**, 10156; (h) V. Chandrasekhar, R. Azhakar, B. Murugesapandian, T. Senapati, P. Bag, M. D. Pandey, S. K. Maurya and D. Goswami, *Inorg. Chem.*, 2010, **49**, 4008; (i) V. Chandrasekhar, R. Azhakar, B. Murugesapandian, T. Senapati, P. Bag, M. D. Pandey, S. K. Maurya and D. Goswami, *Inorg. Chem.*, 2010, **49**, 4008; (j) V. Chandrasekhar, T. Senapati, A. Dey and E. C. Sañudo, *Inorg. Chem.*, 2011, **50**, 1420; (k) V. Chandrasekhar, T. Senapati, A. Dey, S. Das, M. Kalisz and R. Clérac, *Inorg. Chem.*, 2012, **51**, 2031; (l) T. Senapati, C. Pichon, R. Ababei, C. Mathonière and R. Clérac, *Inorg. Chem.*, 2012, **51**, 3796. (m) V. Chandrasekhar, T. Senapati and E. C. Sañudo, *Inorg. Chem.*, 2008, **47**, 9553; (n) V. Chandrasekhar, T. Senapati, E. C. Sañudo and R. Clérac, *Inorg. Chem.*, 2009, **48**, 6192.

² (a) Y.-B. Dong, T. Sun, J.-P. Ma, X.-X. Zhao and R.-Q. Huang, *Inorg. Chem.*, 2006, **45**, 10613; (b) P. Yang, J.-J. Wu, H.-Y. Zhou and B.-H. Ye, *Cryst. Growth Des.*, 2012, **12**, 99; (c) Y.-B. Dong, J.-Y. Cheng, H.-Y. Wang, R.-Q. Huang, B. Tang, M. D. Smith and H.-C. Z. Loye, *Chem. Mater.*, 2003, **15**, 2593.

³ (a) F. Barigelletti, L. Flamigni, *Chem. Soc. Rev.*, 2000, **29**, 1; (b) H. Wang, S. Mauthoor, S. Din, J. A. Gardener, R. Chang, M. Warner, G. Aeppli, D. W. McComb, M. P. Ryan, W. Wu, A. J. Fisher, M. Stoneham and S. Heutz, *Acsnano*. 2010, **4**, 3921; (c) T.-Y. Dong, S.-W. Chang, S.-F. Lin, M.-C. Lin, Y.-S. Wen, L. Lee, *Organometallics* 2006, **25**, 2018; (e) T.-Y. Dong, H.-W. Shih, L.-S. Chang, *Langmuir* 2004, **20**, 9340.

⁴ (a) C. Copÿret, M. Chabanas, R. P. Saint-Arroman and J.-M. Basset, *Angew. Chem. Int. Ed.*, 2003, **42**, 156; (b) S.M. Lang and T. M. Bemhudt, *Phys. Chem. Chem. Phys.*, 2012, **14**, 9255; (c) D. S. Nesterov, E. N. Chygorin, V. N. Kokozay, V. V. Bon, R. Boča, Y. N. Kozlov, L. Shulpin, S. J. Jezierska, A. Ozarowski, A. J. L. Pombeiro and G. B. Shulpin, *Inorg. Chem.*, 2012, **51**, 9110; (d) K.-I. Shimizu, K. Shimura, M. Nishimurab, A. Satsuma, *RSC Advances*, 2011, **1**, 1310; (e) Y. Li, J. H.-C. Liu, C. A. Witham, W. Huang, M. A. Marcus, S. C. Fakra, P. Alayoglu, Z. Zhu, C. M. Thompson, A. Arjun, K. Lee, E. Gross, F. D. Toste and G. A. Somorjai, *J. Am. Chem. Soc.*, 2011, **133**, 13527.

⁵ (a) R. T. W. Scott, L. F. Jones, I. S. Tidmarsh, B. Breeze, R. H. Laye, J. Wolowska, D. J. Stone, A. Collins, S. Parsons, W. Wernsdorfer, G. Aromi, E. J. L. McInnes and E. K. Brechin, *Chem. Eur. J.*, 2009, **15**, 12389; (b) Y.-L. Zhou, M.-H. Zeng, X.-C. Liu, H. Liang and M. Kurmoo, *Chem. Eur. J.*, 2011, **17**, 1408; (c) J.-Y. Xu, H.-B. Song, G.-F. Xu, X. Qiao, S.-P. Yan, D.-Z. Liao, Y. Journaux and J. Cano, *Chem. Commun.*, 2012, **48**, 1015; (d) S. T. Ochsenbein, M. Murrie, E. Rusanov, H. Stoeckli-Evans, C. Sekine and H. U. GuIdel, *Inorg. Chem.* 2002, **41**, 5133; (e) A. Bell, G. Aromi', S. J. Teat, W. Wernsdorferd and R. E. P. Winpenny, *Chem. Commun.*, 2005, 2808; (f) A. Ferguson, A. Parkin, J. Sanchez-Benitez, K. Kamenev, W. Wernsdorfer and M. Murrie, *Chem. Commun.* 2007, 3473; (g) M. Murugesu, J. Raftery, W. Wernsdorfer, G. Christou and E. K. Brechin, *Inorg. Chem.*, 2004, **43**, 4203.

⁶ (a) H. Ke, P. Gamez, L. Zhao, G.-F. Xu, S. Xue, J. Tang, *Inorg. Chem.*, 2010, **49**, 7549; (b) Y.-N. Guo, X.-H. Chen, S. Xue, J. Tang, *Inorg. Chem.*, 2011, **50**, 9705; (c) S. Petit, P. Neugebauer, G. Pilet, G. Chastanet, A.-L. Barra, A. B. Antunes, W. Wernsdorfer, D. Luneau, *Inorg. Chem.*, 2012, **51**, 6645; (d) Y. Ma, G.-F. Xu, X. Yang, L.-C. Li, J. Tang, S.-P. Yan, P. Chenga and D.-Z.

Liao, *Chem. Commun.*, 2010, **46**, 8264; (f) G.-F. Xu, Q.-L. Wang, P. Gamez, Y. Ma, R. Cle´rac, J. Tang, S.-P. Yan, P. Cheng and D.-Z. Liao, *Chem. Commun.*, 2010, **46**, 1506.

⁷ (a) T. C. Stamatatos, A. Escuer, K. A. Abboud, C. P. Raptopoulou, S. P. Perlepes and G. Christou, *Inorg. Chem.*, 2008, **47**, 11825; (b) D. I. Alexandropoulos, C. Papatriantafyllopoulou, G. Aromi, O. Roubeau, S. J. Teat, S. P. Perlepes, G. Christou and T. C. Stamatatos, *Inorg. Chem.*, 2010, **49**, 3962; (c) T. C. Stamatatos, K. A. Abboud, S. P. Perlepes and G. Christou, *Dalton Trans.*, 2007, **35**, 3861; (d) M. Murugesu, K. A. Abboud and G. Christou, *Polyhedron.*, 2004, **23**, 2779; (e) K. F. Konidaris, V. Bekiari, E. Katsoulakou, C. P. Raptopoulou, V. Psycharis, E. Manessi-Zoupa, G. E. Kostakis and S. P. Perlepes, *Dalton Trans.* **2012**, *41*, 3797; (f) T. Stamatatos, C. Papatriantafyllopoulou, E. Katsoulakou, C. P. Raptopoulou and S. P. Perlepes, *Polyhedron* 2007, **26**, 1830; (g) B. Biswas, S. Salunke-Gawali, T. Weyhermuller, V. Bachler, Eckhard. Bill and P. Chaudhuri, *Inorg. Chem.*, 2010, **49**, 626; (h) P. Chaudhuri, T. Weyhermueller, R. Wagner, S. Khanra, B. Biswas, E. Bothe and E. Bill, *Inorg. Chem.*, 2007, **46**, 9003; (i) S. Ross, T. Weyhermueller, E. Bill, K. Wiegardt and P. Chaudhuri, *Inorg. Chem.*, 2001, **40**, 6656; (j) J. Esteban, L. Alcazar, M. Torres-Molina, M. Monfort, M. Font-Bardia and A. Escuer, *Inorg. Chem.*, 2012, **51**, 5503; (k) J. Esteban, E. Ruiz, M. Font-Bardia, T. Calvet and A. Escuer, *Chem. Eur. J.*, 2012, **18**, 3637.

⁸ (a) H. -L. Tsai, C. -I. Yang, W. Wernsdorfer, S. -H. Huang, S.-Y. Jhan, M. -H. Liu and G. -H. Lee, *Inorg. Chem.*, 2012, **51**, 13171; (b) C. -I. Yang, W. Wernsdorfer, G. -H. Lee and H. -L. Tsai, *J. Am. Chem. Soc.*, 2007, **129**, 456; (c) C. -I. Yang, W. Wernsdorfer, K. -H. Cheng, M. Nakano, G. -H. Lee and H. -L. Tsia, *Inorg. Chem.*, 2008, **47**, 10184; (d) C. -I. Yang, Y. -J. Tsai, S. -P. Hung, H. -L. Tsai and M. Nakano, *Chem. Commun.*, 2010, **46**, 5716; (e) L. F. Jones, A. Prescimone, M. Evangelisti and E. K. Brechin, *Chem. Commun.*, 2009, 2023.

⁹ (a) A. Escuer, J. Esteban, N. Aliaga-Alcalde, M. Font-Bardia, T. Calvet, O. Roubeau and S. J. Teat, *Inorg. Chem.*, 2010, **49**, 2259; (b) A. Escuer, J. Esteban and O. Roubeau, *Inorg. Chem.*, 2011, **50**, 8893; (c) A. Escuer, B. Cordero, M. Font-Bardia, T. Calvet, O. Roubeau, S. J. Teat, S. Fedi and F. Fabrizi de Biani, *Dalton Trans.*, 2010, **39**, 4817.

¹⁰ (a) V. Chandrasekhar, B. M. Pandian, J. J. Vittal and R. Clerac, *Inorg. Chem.*, 2009, **48**, 1148; (b) H. Ke, L. Zhao, Y. Guo and J. Tang, *Inorg. Chem.*, 2012, **51**, 2699; (c) Y. Gao, L. Zhao, X. Xu, G.-F. Xu, Y.-N. Guo, J. Tang and Z. Liu, *Inorg. Chem.* **2011**, *50*, 1304; (d) K. C. Mondal, G. E. Kostakis, Y. Lan, W. Wernsdorfer, C. E. Anson and A. K. Powell, *Inorg. Chem.*, 2011, **50**, 11604; (e) C. G. Efthymiou, T. C. Stamatatos, C. Papatriantafyllopoulou, A. J. Tasiopoulos, W. Wernsdorfer, S. P. Perlepes and G. Christou, *Inorg. Chem.* 2010, **49**, 9737; (f) K. C. Mondal, A. Sundt, Y. Lan, G. E. Kostakis, O. Waldmann, L. Ungur, L. F. Chibotaru, C. E. Anson and A. K. Powell, *Angew. Chem. Int. Ed.*, 2012, **51**, 7550; (g) F. Mori, T. Nyui, T. Ishida, T. Nogami, K.-Y. Choi and H. Nojiri, *J. Am. Chem. Soc.*, 2006, **128**, 1440; (h) O. Iasco, G. Novitchi, E. Jeanneau, W. Wernsdorfer and D. Luneau, *Inorg. Chem.*, 2011, **50**, 7373; (i) S. K. Langley, L. Ungur, N. F. Chilton, B. Moubaraki, L. F. Chibotaru and S. K. Murray, *Chem. Eur. J.*, 2011, **17**, 9209; (j) C. Papatriantafyllopoulou, W. Wernsdorfer, K. A. Abboud and G. Christou, *Inorg. Chem.*, 2011, **50**, 421; (k) J.-L. Liu, F.-S. Guo, Z.-S. Meng, Y.-Z. Zheng, J.-D. Leng, M.-L. Tong, L. Ungur, L. F. Chibotaru, K. J. Heroux and D. N. Hendrickson, *Chem. Sci.*, 2011, **2**, 1268; (l) A. Saha, M. Thompson, K. A. Abboud, W. Wernsdorfer and G. Christou, *Inorg. Chem.*, 2011, *50*, 10476.

¹¹ (a) Vogel's Text Book of Practical Organic Chemistry, 5th ed.; B. S. Furniss, A. J. Hannaford, P. W. G. Smith, A. R. Tatchell, Eds. ELBS and Longman: London, U.K., 1989. (b) D. B. G. Williams and M. Lawton, *J. Org. Chem.* 2010, **75**, 8351.

-
- ¹² G. Tallec, D. Imbert, P. H. Fries and M. Mazzanti, *Dalton Trans.*, 2010, **39**, 9490.
- ¹³ A. D. Becke, *Physical Review A*, 1988, **38**, 3098.
- ¹⁴ A. D. Becke, *Journal of Chemical Physics*, 1993, **98**, 5648.
- ¹⁵ C. T. Lee, W. T. Yang, R. G. Parr, *Physical Review B*, 1988, **37**, 785.
- ¹⁶ M. J. Frisch et al.; Gaussian 09 (Revision B.01) ed.; Gaussian, Inc: Pittsburgh, PA, 2009.
- ¹⁷ K. J. Barnham, E. C. L. Gautier, G. B. Kok, G. Krippner, *U.S. Pat. Appl. Publ.*, 2008, US 20080161353 A1 2008
- ¹⁸ (a) SMART & SAINT Software Reference manuals, Version 6.45; Bruker Analytical X-ray Systems, Inc.; Madison, WI, 2003; (b) G. M. Sheldrick, SADABS a software for empirical absorption correction, Ver. 2.05; University of Göttingen: Göttingen, Germany, 2002; (c) G. M. Sheldrick, SHELXTL, Version 6.12; Bruker AXS Inc: Madison, WI, 2001; (d) G. M. Sheldrick, SHELXL97, Program for Crystal Structure Refinement; University of Göttingen: Göttingen, Germany, 1997.
- ¹⁹ K. Bradenburg, Diamond, version 3.1e; Crystal Impact GbR: Bonn, Germany, 2005.
- ²⁰ C. Papatriantafyllopoulou, T. C. Stamatatos, C. G. Efthymiou, L. Cunha-Silva, F. A. Almeida Paz, S. P. Perlepes and G. Christou, *Inorg. Chem.*, 2010, **49**, 9743.
- ²¹ R. A. Coxall, S. G. Harris, D. K. Henderson, S. Parsons, P. A. Tasker and R. E. P. Winpenny, *J. Chem. Soc., Dalton Trans.*, 2000, 2349.
- ²² (a) J. L. Sanz, R. Ruiz, A. Gleizes, F. Lloret, J. Faus, M. Julve, Y. Journaux, *Inorg. Chem.*, 1996, **35**, 7384; (b) A. Figuerola, C. Diaz, J. Ribas, V. Tangoulis, J. Granell, F. Lloret, M. Maestro, *Inorg. Chem.*, 2003, **42**, 641; (c) J. Vallejo, J. Cano, I. Castro, M. Julve, F. Lloret, O. Fabelo, L. Cañadillas-Delgado, E. Pardo *Chem. Commun.*, 2012, **48**, 7726.